ChemPubSoc Europe

DOI: 10.1002/cphc.201701264

CHEMPHYSCHEM Articles

Micropolarity and Hydrogen-Bond Donor Ability of Environmentally Friendly Anionic Reverse Micelles Explored by UV/Vis Absorption of a Molecular Probe and FTIR Spectroscopy

Valeria R. Girardi, Juana J. Silber, Ruben Darío Falcone,* and N. Mariano Correa[a]

In the present work we show how two biocompatible solvents, methyl laurate (ML) and isopropyl myristate (IPM), can be used as a less toxic alternative to replace the nonpolar component in a sodium 1,4-bis-2-ethylhexylsulfosuccinate (AOT) reverse micelles (RMs) formulation. In this sense, the micropolarity and the hydrogen-bond ability of the interface were monitored through the use of the solvatochromism of a molecular probe (1-methyl-8-oxyquinolinium betaine, QB) and Fourier transform infrared spectroscopy (FTIR). Our results demonstrate that the micropolarity sensed by QB in ML RMs is lower than in IPM RMs. Additionally, the water molecules form stronger H-bond interactions with the polar head of AOT in ML than in IPM. By FTIR was revealed that more water molecules interact with the interface in ML/AOT RMs. On the other hand, for AOT RMs generated in IPM, the weaker water–surfactant interaction allows the water molecules to establish hydrogen bonds with each other trending to bulk water more easily than in ML RMs, a consequence of the dissimilar penetration of nonpolar solvents into the interfacial region. The penetration process is strongly controlled by the polarity and viscosity of the external solvents. All of these results allow us to characterize these biocompatible systems, providing information about interfacial properties and how they can be altered by changing the external solvent. The ability of the nontoxic solvent to penetrate or not into the AOT interface produces a new interface with attractive properties.

1. Introduction

Reverse micelles (RMs) are a class of self-assemblies system generally described as nanometer sized water droplets dispersed in a nonpolar solvent with the aid of a surfactant monolayer.[1,2] Polar and nonpolar substances can be solubilized by RMs and this ability confer to them several applications in fields such as chemical and enzymatic reactions,[2] nanomaterials synthesis,[3–7] in drug delivery systems,[8] among others. Different kinds of surfactants (anionic, cationic and nonionic) have been used to formulate RMs in nonpolar solvents. Particularly, the surfactant most employed is the anionic sodium 1,4-bis-2-ethylhexylsulfosuccinate (AOT, Scheme 1).[2,3,9–14] This surfactant has the ability to forms spherical RMs in aromatic and aliphatic nonpolar solvents without the addition of a cosurfactant and, variable amount of water (quantified as $W_0 = [H_2O]/[Surfactant]$) can be solubilized depending on the chemical nature of the external solvent and temperature, among other factors.[9] Even that RMs have been explored and characterized since several decades ago, actually the main critical problem is still the potential toxicity of their components; particularly the

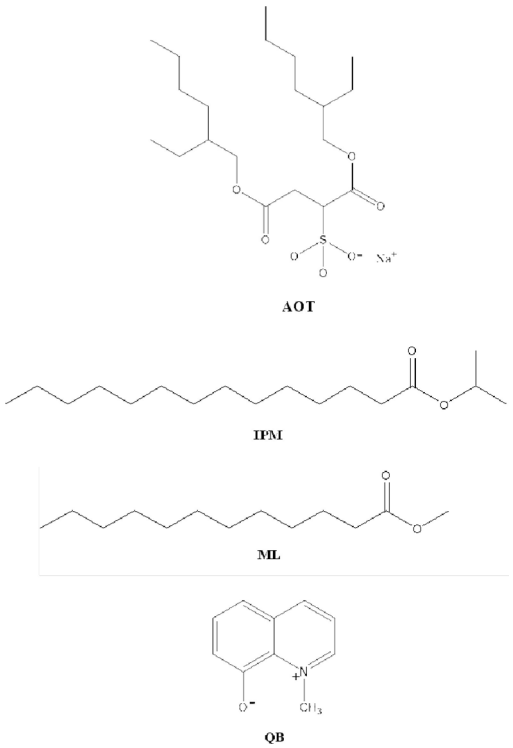

Scheme 1. Molecular structures of AOT, IPM, ML and QB.

[a] *Dr. V. R. Girardi, Prof. J. J. Silber, Dr. R. D. Falcone, Dr. N. M. Correa*
Departamento de Química
Universidad Nacional de Río Cuarto
Agencia Postal # 3, C.P. X5804BYA Río Cuarto (Argentina)
E-mail: rfalcone@exa.unrc.edu.ar

Supporting Information and the ORCID identification number(s) for the author(s) of this article can be found under: https://doi.org/10.1002/cphc.201701264.

external solvent which is the major component in the solution. This difficulty reduces their potential application in industries such as food, cosmetic, and pharmaceutical. In these sense, many efforts have been made to formulate non-toxic RMs created in different oils. In particular, RMs prepared in biocompatible solvents such as isopropyl myristate (IPM, Scheme 1), ethyl myristate, ethyl palmitate and ethyl oleate appears as promising replacement to traditional nonpolar solvents.[10,15–18] These long chain fatty acid esters are environmentally friendly with low toxicity and highly biodegradable.[15,19–21] One of the main goals is to produce non-toxic RMs that preserves the unique properties of the very-well known AOT RMs in traditional solvents.

Previous studies performed in our group[18] have shown a peculiar and unexpected behavior of the AOT RMs formed in methyl laurate (ML, Scheme 1), in comparison with the RMs formulated in IPM despite the similar chemical structure of these external solvents. Thus, it was observed that the anionic surfactant is completely soluble in both solvents in absence of water ($W_0 = 0$). The maximum amount of water dissolved (defined as W_0^{max}) for both RMs were different being, the ML/AOT RMs able to dissolve approximately the double amount of water than IPM/AOT. From the dynamic light scattering (DLS) experiments, was observed an increase in the diameter of the droplets (d_{app}) when the W_0 increases in IPM and ML RMs, proving that the RMs are formed, hence the water molecules are effectively entrapped by the AOT layer. However, the sizes were dissimilar between both RMs. For instance, at $W_0 = 10$ the d_{app} value for IPM/AOT RMs was 3.1 nm but 7 nm in the case of ML/AOT RMs. The aggregation numbers (N_{agg}) of both RMs were also very different. A N_{agg} of 49 was obtained for IPM/AOT/water RMs at $W_0 = 15$, being around 182 for ML/AOT/water. Interestingly, we observed similarities between these biocompatible solvents and those traditionally used to create RMs such as *n*-heptane and benzene. In this sense, the W_0^{max} values observed in ML/AOT and *n*-heptane/AOT were quite similar and, for IPM/AOT and benzene/AOT only slightly different but both are able to dissolve less water than ML/AOT or *n*-heptane/AOT RMs.[4,22] Additionally, the similar N_{agg} values obtained for IPM/AOT/water and benzene/AOT/water,[23] around 30, and for ML/AOT/water and *n*-heptane/AOT/water[24] around 180 reinforces the idea that IPM and ML have analogous behavior in AOT RMs that benzene and *n*-heptane, respectively.

In order to explore more in detail on the unique microenvironment created in these RMs, we investigate the water entrapped inside IPM/AOT and ML/AOT RMs by using two approaches: i) absorption spectroscopy using 1-methyl-8-oxyquinolinium betaine (QB, Scheme 1) as molecular probe; and ii) Fourier transform infrared spectroscopy (FTIR).

Experimental

Materials

Sodium 1,4-bis (2-ethylhexyl) sulfosuccinate (AOT) from Sigma (> 99% purity), was dried under vacuum prior use. Isopropyl myristate (IPM) and methyl laureate (ML) both from Sigma (> 98% purity), were stored over molecular sieves before use. Ultrapure water was obtained from Labonco equipment model 90901-01.

1-methyl-8-oxyquinolinium betaine (QB) was synthesized according to the procedure reported by Ueda and Schelly.[25]

Methods

The stock solutions of AOT in IPM and ML were prepared by mass and volumetric dilution. Aliquots of these stock solutions were used to make individual RMs solutions with different amount of water, defined as $W_0 = [water]/[AOT]$. The incorporation of water into each micellar solutions were performed using calibrated microsyringes. To obtain optically clear solutions they were shaken in a sonicating bath.

For the absorption experiments, a 1×10^{-2} M solution of QB in methanol (Sintorgan HPLC quality) was prepared. The appropriate amount of this solution to obtain a concentration of 3×10^{-4} M for QB in the AOT RMs was transferred into a volumetric flask, and the methanol was evaporated by bubbling dry N_2; then, the surfactant RMs stock solution was added to the residue and agitated in a sonicating bath until the RMs was optically clear. For the experiments varying the AOT concentration at W_0 constant (0 and 10), a stock solution of surfactant 0.2 M was used. Thus, to the cell baring 2 mL of QB of the same concentration in the nonpolar solvent, was added the appropriate amount of surfactant and molecular probe stock solution to obtain a given concentration of surfactant in the micellar media. Therefore, the absorbance values of the molecular probe were not affected by dilution. For the experiments varying the water content, an AOT RMs solution prepared at [AOT] = 0.1 M was employed.

For FTIR experiments, monodeuterated water (HOD) as polar phase was used, which was prepared by stirring a solution of 10% D_2O (> 99% purity from Sigma) in H_2O at room temperature for 1 h in order to allow the exchange of H.[26]

General

UV/Vis absorption spectra were recorded using a spectrophotometer Shimadzu 2401 with a thermostated sample holder. The path length used in absorption experiments was 1 cm. All experimental points were measured three times with different prepared samples.

FTIR spectra were recorded with a Nicolet IMPACT 400 spectrometer. The FTIR measurements for the RMs samples were taken in Irtran-2 cell of 0.5 mm path length from Wilmad Glass (Buena, NJ). FTIR spectra were obtained by co-adding 200 spectra at a resolution of 0.5 cm^{-1}. The ν_{OD} spectral band of HOD was superimposed on a finite background. It was assumed that this background could be approximated with the spectrum of 100% H_2O in the ν_{OD} spectral region.[26] Therefore the reference sample, at each W_0 values, was a surfactant solu-

tion containing exactly the same W_0 but adjusted with pure H_2O.

All the experiments were carried out at 25±0.5 °C.

2. Results and Discussion

2.1. QB in Nontoxic Lipophilic Solvents/AOT Reverse Micelles

We have chosen QB as molecular probe because its solvatochromic behavior is highly sensitive to the microenvironment[27–29] and, it was previously used to obtain valuable information about aqueous and nonaqueous AOT RMs.[14,27,28,30] QB has an UV-visible absorption spectrum with two electronic absorption bands: an absorption band in the visible region, B_1, that is primarily sensitive to polarity, and another band peaking at shorter wavelength in the UV, B_2, which reflects the hydrogen bond donor capability of the solvent.[27,28] The absorbance of the B_2 band is highly sensitive to the molecule's environment hence, the absorbance ratio of B_2 to B_1 bands (Abs B_2/Abs B_1), in combination with the absorption bands shifts, provides an effective method to determine the properties of the microenvironment surrounding the probe.[14,27,28,30]

In the present contribution, the QB behavior in non-toxic lipophilic solvents/AOT RMs was explored, performing all the experiments at different surfactant concentration; first in absence of water addition ($W_0=0$) and later in presence of the entrapped water ($W_0=10$). Finally, the variation of the water content when the RMs is formed ([AOT] = 0.1 M) was investigated.

2.1.1. QB in IPM/AOT RMs

Figure 1 shows the QB absorption spectra in IPM/AOT RMs varying [AOT] at [QB] = 3×10^{-4} M and $W_0=0$. As QB is soluble in pure IPM, the surfactant concentration was varied from 0 (pure non-polar solvent) to 0.2 M. In Figure 2 A and B are plotted the absorption maximum of B_1 and B_2 bands when the surfactant concentration is increased, respectively.

As evident in Figures 2 A, B, there are hypsochromic shifts of B_1 and B_2 bands when the [AOT] increases. However, at [AOT]

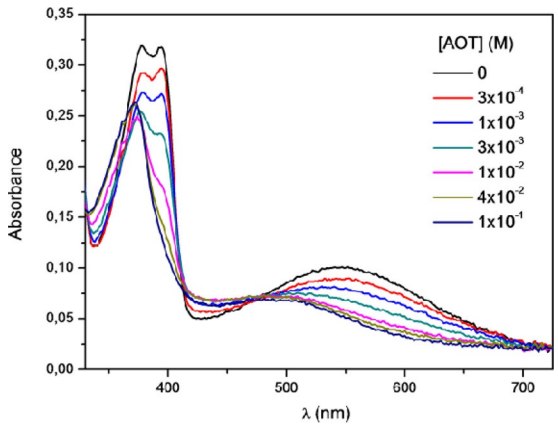

Figure 1. QB absorption spectra in IPM/AOT RMs as a function of AOT concentration at $W_0=0$. [QB] = 3×10^{-4} M.

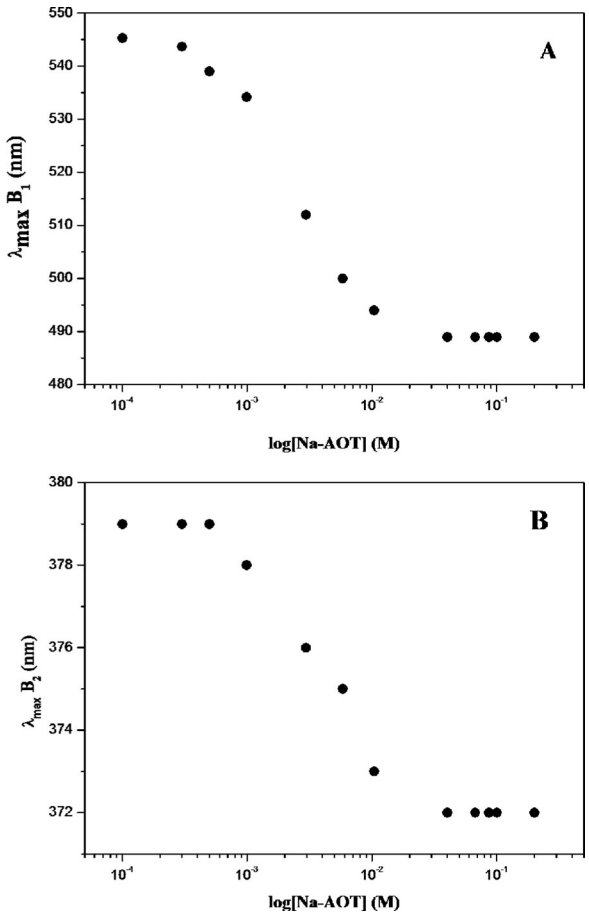

Figure 2. Variation of the B_1 band maximum (A) and the B_2 band maximum (B) of QB in IPM/AOT RMs as a function of AOT concentration at $W_0=0$. [QB] = 3×10^{-4} M.

$>10^{-3}$ M the absorption values remain practically constant. This behavior may denote that the QB microenvironment is not changing after the RMs formation. As the location of the probe is crucial to infer RMs properties and, as QB is soluble in the non-polar solvent, when the micelle is formed (concentrations above the CMC) QB can undergo a partition process between the two different pseudophases: the RMs interface and the non-polar organic solvent, changing the surfactant concentration.[28] Figure 1 shows that there is no isosbestic point for QB spectra in IPM/AOT RMs at $W_0=0$ and, Figures 2A, B clearly show the lack of spectral changes at [AOT] $>10^{-3}$ M. Both facts suggest that, even in absence of water, QB is anchored to the interface and the partition process between the two pseudophases is negligible. Additionally, the CMC value (4.2×10^{-3} M) for the IPM/AOT RMs can be obtained from the inflection point of data plotted in Figure S1 in the Supporting Information. Similar plots were obtained in all the systems explored (results not shown).

The variation of the QB absorption spectra as a function of [AOT] in presence of water added in the IPM/AOT RMs is potted in Figure S2. Figures S3 A–B summarize the λ_{max} B_1 and λ_{max} B_2 values for QB in IPM/AOT/water RMs, respectively, varying [AOT] at $W_0=10$. For comparison, the λ_{max} B_1 values varying the surfactant concentration at $W_0=0$ and 10 are present-

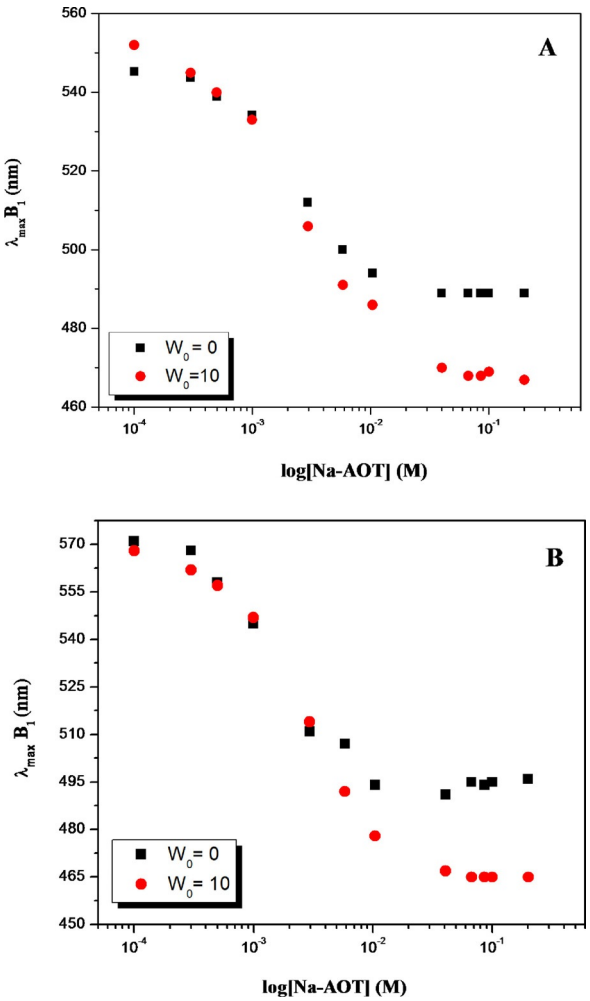

Figure 3. Variation of the B_1 band maximum of QB in IPM/AOT/water (A) and ML/AOT/water (B) RMs as a function of AOT concentration at $W_0 = 0$ and 10. [QB] = 3×10^{-4} M.

ed in Figure 3A. As it can be observed, the presence of water entrapped in the RMs modified the spectral behavior of QB. Even that the tendencies are similar to the system at $W_0 = 0$, that is, shifting to lower wavelengths when the surfactant concentration increases, at $W_0 = 10$ the micropolarity sensed by QB is larger (red points in Figure 3A) that the media in absence of water (black points in Figure 3A). This difference denotes that the molecular probe senses the water at the interface.[27]

2.1.2. QB in ML/AOT RMs

Similar experiments were performed for QB in ML/AOT RMs. Thus, in Figures S4–S7 are plotted the spectra of QB, the B_1 and B_2 maximum values as a function of [AOT] at $W_0 = 0$ and 10. Figure 3B summarizes the λ_{max} B_1 values varying the surfactant concentration at $W_0 = 0$ and 10. Additionally, in Table S1 are shown the CMC values obtained for both systems. It is important to note that all CMC values are comparable to those reported for AOT RMs formulated in solvents such as benzene or *n*-heptane.[14,28] Moreover, the presence of water ($W_0 = 10$) in both biocompatible systems help to organize the RMs at lower surfactant concentration (low CMC) than at $W_0 = 0$.

The results observed in Figure 3B indicate an increment on the micropolarity sensed by QB in ML/AOT RMs when the surfactant concentration increases. Moreover, when W_0 increases QB is sensing the presence of water at the interface.[27]

In order to make comparison between both biocompatible systems and conventional AOT RMs and, to understand the influence of the external solvent on the properties of the RMs studied we have decided to compare the results at [AOT] = 0.1 M, which is above the value of the CMC. In Table 1 are gathered the values of λ_{max} B_1 values for QB in IPM/AOT/water and ML/AOT/water RMs at [AOT] = 0.1 M at $W_0 = 0$ and 10. The spectroscopic values for QB in neat IPM, ML and water are also shown in Table 1.

Table 1. Maxima absorption wavelength of B_1 values of QB in different systems. [QB] = 3×10^{-4} M; [AOT] = 0.1 M.

System	λ_{max} B_1 [nm] $W_0 = 0$	$W_0 = 10$
IPM/AOT	490	465
ML/AOT	496	468
neat IPM	552	
neat ML	573	
neat water [a]	441	

[a] Data obtained from Refs. [27,28].

Analyzing the QB λ_{max} B_1 values data gathered in Table 1 it can be seen that the λ_{max} B_1 value is smaller for IPM/AOT than for ML/AOT at $W_0 = 0$. This suggests that the micropolarity of the interface is higher in the former system. When water is added to both RMs, the micropolarity sensed by QB in ML RMs is still lower than in IPM RMs.

In comparison with traditional non-polar external solvents, QB detects differences between both biocompatible solvents and *n*-hexane or benzene. For example, at $W_0 = 0$ the λ_{max} B_1 appears at 506 nm and 510 nm in *n*-hexane/AOT and benzene/AOT RMs, respectively.[28] Table 1 shows a λ_{max} B_1 value of 490 nm and 496 nm for AOT RMs formed in IPM and ML, respectively. Even that the micropolarity in benzene/AOT RMs is lower than in *n*-hexane/AOT RMs (same tendency that IPM and ML RMs), both traditional solvents produce different interfacial microenvironment that the biocompatible solvents.

In order to provide more information about the influence of the external solvent on the water entrapped in both RMs, we varied the water content at fixed [AOT]. Figures S8 and S9, show the QB absorption spectra with varying W_0 in IPM/AOT/water and ML/AOT/water RMs, respectively. The spectral changes of QB show that both bands undergo hypsochromic shifts when the amount of water increases. On the other hand, it is very interesting to analyze the $AbsB_2/AbsB_1$ ratio values as a function of W_0 since this is only sensitive to the H-bond ability of the environment.[14,27,28,30] Figure 4 summarizes the $AbsB_2/AbsB_1$ ratio values for QB in IPM/AOT/water and ML/AOT/water RMs.

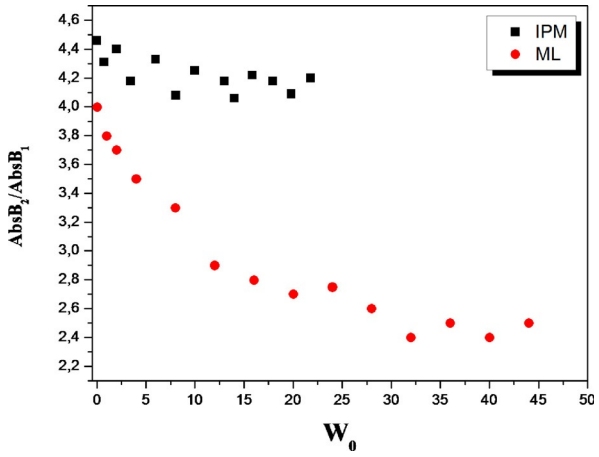

Figure 4. Variation of the absorbance ratio between B_2 and B_1 bands of QB in IPM/AOT/water and ML/AOT/water RMs as a function of W_0. [QB] = 3×10^{-4} M. [AOT] = 0.1 M.

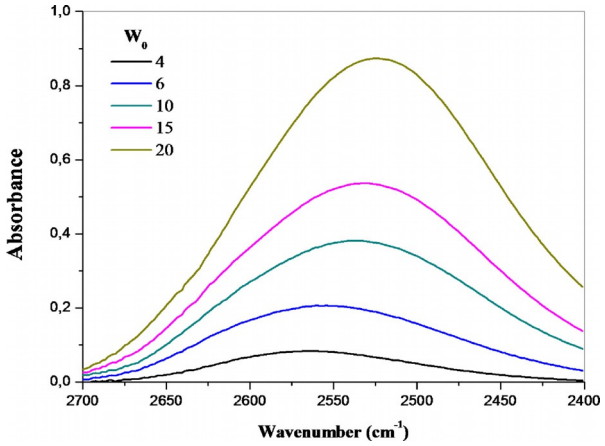

Figure 5. FTIR spectra in the region of O-D stretching frequency of HOD in IPM/AOT/water RMs upon increasing the W_0 values. The IPM bands have been subtracted. [AOT] = 0.1 M.

Figure 4 shows two different profiles when W_0 increase in both RMs. The $AbsB_2/AbsB_1$ values are practically constant in the IPM RMs but there is a significant diminishing in the values with the increasing of the water content in the ML RMs. The data for IPM RMs suggests a very poor interaction by H-bond interaction between QB and water molecules at the interface. On the other hand, the results observed in ML system are consistent with an important H-bond donor ability of the region around the molecular probe. At the W_0 maximum value reached, QB detects an $AbsB_2/AbsB_1$ value equal to 2.4 in ML/AOT/water, while for IPM/AOT/water RMs, the ratio value is around 4. Particularly, this last value is quite far from that found in pure water ($AbsB_2/AbsB_1 = 1.1$).[28] Apparently, these results denote that water forms stronger H-bond interaction with the polar head of AOT in ML than in IPM. Consequently, the structure of the interfacial water in IPM/AOT RMs should be different from those found in the ML/AOT RMs.

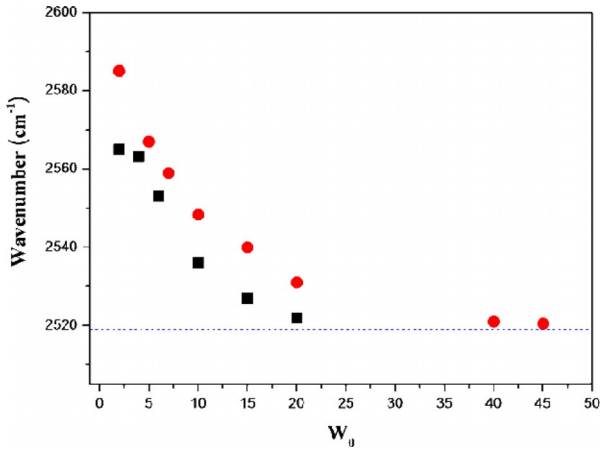

Figure 6. Shift of O-D stretching frequency for HOD upon increasing the W_0: IPM/AOT/HOD (■) and ML/AOT/HOD (●). The ν_{OD} value for pure HOD (–) is included for comparison. [AOT] = 0.1 M.

2.2. Nontoxic Lipophilic Solvents/AOT/Water Reverse Micelles Explored by FTIR

To gain more insights about the biocompatible RMs and the water-surfactant interaction we investigated the systems using the noninvasive technique FTIR spectroscopy, which allows us to infer, for example, interactions existing at the interface.[31,32] As it was performed in previous works[26,31,32] we use monodeuterated water as polar phase in our RMs. Thus, we follow the water O-D stretching mode (ν_{OD}) in the AOT RMs. It must be pointed out that the main stretching bands corresponding to AOT (C=O, symmetrical and asymmetrical SO_3^-)[26,32,33] cannot be monitored in the RMs formed in these systems since they appear in the same region of the lipophilic ester non-polar solvents.

Figure 5 shows the FTIR spectra in the region corresponding to the O-D stretching band (ν_{OD}) of HOD in IPM/AOT/water system at different W_0 values. In Figure S10 (supporting information section) is shown the corresponding FTIR study obtained in ML/AOT/water RMs. Figure 6 plots the ν_{OD} values as a function of the water content for both RMs.

As can be seen from Figures 5 and S10, for HOD entrapped in IPM/AOT and ML/AOT RMs at all the W_0 values investigated a symmetric band was observed and attributed to only one kind of water present in the RMs. Additionally, from Figure 6 two interesting facts can be observed: i) all the O-D stretching frequency values in both RMs are larger than the corresponding to neat HDO (2519 cm^{-1})[34] specially at low W_0 and, ii) the $\nu_{O\text{-}D}$ values at the same water content are different between both RMs.

The $\nu_{O\text{-}D}$ values larger than neat water observed when this polar solvent is entrapped in both non-toxic RMs, suggest that water molecules are interacting with the surfactant at the interface breaking its H-bond network.[31,32] This is probably due to the interaction mainly with the polar heads group (SO_3^-) of AOT.[31,32]

Figure 6 also shows that although in both RMs the $\nu_{O\text{-}D}$ values shift to lower frequencies as W_0 increases, the values obtained are different from each other. For example, at $W_0 = 2$

in IPM RMs the frequency of the O-D band appears at 2565 cm^{-1}, while in RMs formed in ML the $\nu_{O\text{-}D}$ value is 2585 cm^{-1}. The same tendency is observed at $W_0 = 10$; being the band at 2536 cm^{-1} in IPM and at 2548 cm^{-1} in ML RMs. These results suggest a difference in the magnitude of the water-anionic surfactant interaction at the interface. In comparison with traditional non-polar solvents, the O-D stretching mode of the water entrapped also show similarities with the biocompatible solvents explored here. For example, in benzene/AOT RMs the frequency of the O-D band is 2563 cm^{-1} at $W_0 = 2$.[32] On the other hand, at the same water content but in isooctane/AOT RMs the O-D band appears at 2570 cm^{-1}.[26]

Analyzing the data showed in Figure 6, a stronger water-surfactant interaction is present in ML RMs while for IPM RMs this interaction seems to be weaker. This would lead to more water molecules interacting with the interface in ML/AOT RMs with its H-bond network more disrupted. On the other hand, for AOT RMs generated in IPM a weaker water-surfactant interaction allows the water molecules to establish H-bond to each other trending to bulk water more easily than in ML RMs. These evidences can be produced by the dissimilar penetration of the non-polar solvents into the interfacial region.[18] Two factors can be invoked to explain this phenomenon: the viscosity and polarity of the external solvents.

When more viscous is the solvent, greater is its ability to penetrate to the interface in RMs. For example, common non-polar solvents to create RMs such as benzene and *n*-heptane show this tendency. Benzene is more viscous than *n*-heptane[18] and penetrates more to the interface in AOT.[4] In this sense, the larger viscosity of IPM in comparison with ML[18] allow to penetrate more toward the AOT RMs interface.

As it can be seen from the QB study, IPM is more polar (λ_{max} $B_1 = 552$ nm) than ML (λ_{max} $B_1 = 573$ nm) and consequently can penetrate deeper the polar interface than ML. Furthermore, the IPM penetration into the interfacial zone affect also the H-bond interactions of the region as is reflected by the high value of the $AbsB_2/AbsB_1$ ratio obtained (Figure 4). Thus, the viscosities and polarities of these non-toxic solvents can be invoked to explain why the penetration of IPM into the interface is larger than ML making the interface of IPM/AOT RMs more polar but less H-bonding that ML/AOT RMs.

Thus, upon confinement the water entrapped in IPM RMs seems to be more associated with other water molecules than with the surfactant polar head group. This result is completely different to those found for ML RMs where the confinement makes the interfacial water less self-associated than the bulk one because of the strong water—SO_3^- interaction. In Scheme 2 is represented how the penetration external solvent affect the water structure at the interface in both RMs.

3. Conclusions

The present work demonstrates how two biocompatible solvents can be used to replace non-polar solvent in the AOT RMs formation. Particularly, the polarity and viscosity of the external solvents impact strongly in the interfacial properties of these RMs. All these results allow us to characterize these biocompatible systems, providing information about interfacial properties such as micropolarity and H-bond donor ability and how they can be altered changing the external solvent. Thus, the ability of the non-toxic solvent to penetrate or not into the AOT interface produces a new interface with attractive properties. In this sense, actually we are performing experiments about enzymatic catalysis and nanoparticles synthesis inside IPM and ML AOT RMs. Finally, we demonstrate that the non-toxic AOT RMs systems have similar properties than the traditional AOT RMs made in hydrocarbons. That is, the water is effectively entrapped in the polar interior and, they have different and unique properties in comparison with bulk water.

Acknowledgements

Financial support from the Consejo Nacional de Investigaciones Científicas y Técnicas (PIP CONICET 112–201101-00204, PIP CONICET 112–2015–0100283), Universidad Nacional de Río Cuarto

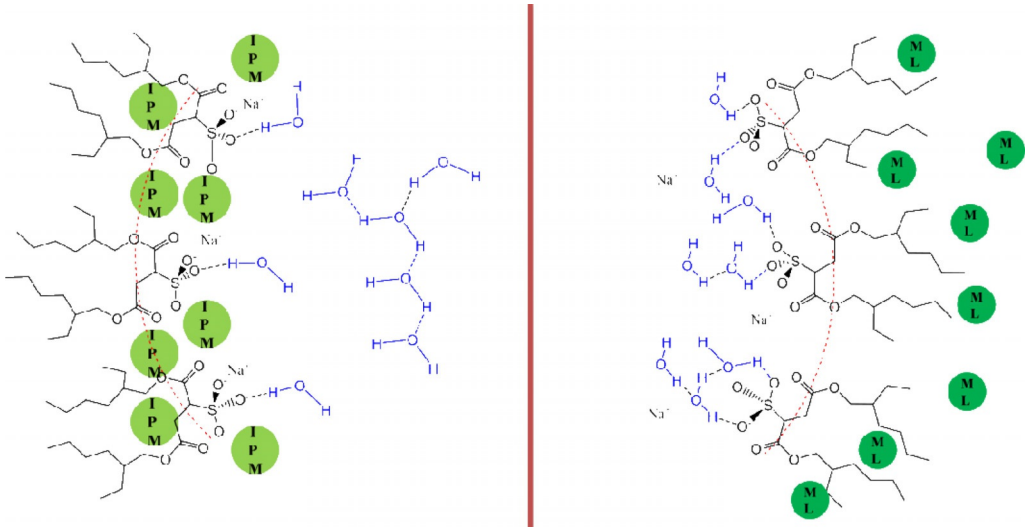

Scheme 2. Schematic representation of the penetration of the IPM (left) and ML (right) in the AOT RMs interfaces.

(PPI-UNRC 2016–2018), Agencia Nacional de Promoción Científica y Técnica (PICT 2012-0232, PICT-2012-0526 and PICT 2015-0585), and Ministerio de Ciencia y Tecnología, gobierno de la provincia de Córdoba (PID 2013) is gratefully acknowledged. J.J.S., N.M.C. and R.D.F. hold a research position at CONICET. V.R.G. thanks CONICET for a research fellowship.

Conflict of Interest

The authors declare no competing financial interests.

Keywords: infrared spectroscopy · reverse micelles · solvent effects · surfactants · water–surfactant interactions

[1] N. Nandi, K. Bhattacharyya, B. Bagchi, *Chem. Rev.* **2000**, *100*, 2013 – 2046.
[2] N. M. Correa, J. J. Silber, R. E. Riter, N. E. Levinger, *Chem. Rev.* **2012**, *112*, 4569 – 4602.
[3] K. Naoe, S. Yoshimoto, N. Naito, M. Kawagoe, M. Imai, *Biochem. Eng. J.* **2011**, *55*, 140 – 143.
[4] J. A. Gutierrez, R. D. Falcone, M. A. Lopez-Quintela, D. Buceta, J. J. Silber, N. M. Correa, *Eur. J. Inorg. Chem.* **2014**, 2095 – 2102.
[5] V. Uskoković, M. Drofenik, *Adv. Colloid Interface Sci.* **2007**, *133*, 23 – 34.
[6] M. S. Orellano, C. Porporatto, J. J. Silber, R. D. Falcone, N. M. Correa, *Carbohydr. Polym.* **2017**, *171*, 85 – 93.
[7] Y. Singh, A. Chandrashekhar, J. G. Meher, K. K. Durga Rao Viswanadham, V. K. Pawar, K. Raval, K. Sharma, P. K. Singh, A. Kumar, M. K. Chourasia, *Eur. J. Pharm. Biopharm.* **2017**, *113*, 198 – 210.
[8] A. Kogan, N. Garti, *Adv. Colloid Interface Sci.* **2006**, *123 – 126*, 369 – 385.
[9] T. K. De, A. Maitra, *Adv. Colloid Interface Sci.* **1995**, *59*, 95 – 193.
[10] X. Zhang, Y. Chen, J. Liu, C. Zhao, H. Zhang, *J. Phys. Chem. B* **2012**, *116*, 3723 – 3734.
[11] M. Appel, T. L. Spehr, R. Wipf, B. Stühn, *J. Colloid Interface Sci.* **2012**, *376*, 140 – 145.
[12] M. Domschke, M. Kraska, R. Feile, B. Stühn, *Soft Matter* **2013**, *9*, 11503.
[13] J. Wei, B. Su, J. Yang, H. Xing, Z. Bao, Y. Yang, Q. Ren, *J. Chem. Eng. Data* **2011**, *56*, 3698 – 3702.
[14] S. S. Quintana, R. D. Falcone, J. J. Silber, N. M. Correa, *ChemPhysChem* **2012**, *13*, 115 – 123.
[15] S. Gupta, S. P. Moulik, *J. Pharm. Sci.* **2008**, *97*, 22 – 45.
[16] M. D. Chatzidaki, K. D. Papavasileiou, M. G. Papadopoulos, A. Xenakis, *Langmuir* **2017**, *33*, 5077 – 5085.
[17] D. Goswami, J. K. Basu, S. De, *Crit. Rev. Biotechnol.* **2013**, *33*, 81 – 96.
[18] V. R. Girardi, J. J. Silber, N. M. Correa, R. D. Falcone, *Colloids Surf. A* **2014**, *457*, 354 – 362.
[19] K. Kundu, A. Das, S. Bardhan, G. Chakraborty, D. Ghosh, B. Kar, S. K. Saha, S. Senapati, R. K. Mitra, B. K. Paul, *Colloids Surf. A* **2016**, *504*, 331 – 342.
[20] K. Kundu, B. K. Paul, *J. Surfactants Deterg.* **2013**, *16*, 865 – 879.
[21] P. Boonme, K. Krauel, A. Graf, T. Rades, V. B. Junyaprasert, *AAPS PharmSciTech* **2006**, *7*, E99 – E104.
[22] D. Grand, *J. Phys. Chem. B* **1998**, *102*, 4322 – 4326.
[23] N. Gorski, Y. M. Ostanevich, *Ber. Bunsen-Ges.* **1990**, *94*, 737 – 741.
[24] J. Lang, A. Jada, A. Malliaris, *J. Phys. Chem.* **1988**, *92*, 1946 – 1953.
[25] M. Ueda, Z. A. Schelly, *Langmuir* **1989**, *5*, 1005 – 1008.
[26] L. P. Novaki, N. M. Correa, J. J. Silber, O. A. El Seoud, *Langmuir* **2000**, *16*, 5573 – 5578.
[27] N. M. Correa, M. A. Biasutti, J. J. Silber, *J. Colloid Interface Sci.* **1995**, *172*, 71 – 76.
[28] N. M. Correa, M. A. Biasutti, J. J. Silber, *J. Colloid Interface Sci.* **1996**, *184*, 570 – 578.
[29] L. P. Novaki, O. A. El Seoud, *Langmuir* **2000**, *16*, 35 – 41.
[30] R. D. Falcone, N. M. Correa, M. A. Biasutti, J. J. Silber, *Langmuir* **2000**, *16*, 3070 – 3076.
[31] E. Odella, R. D. Falcone, J. J. Silber, N. M. Correa, *Phys. Chem. Chem. Phys.* **2014**, *16*, 15457 – 15468.
[32] C. M. O. Lépori, N. M. Correa, J. J. Silber, R. D. Falcone, *Soft Matter* **2016**, *12*, 830 – 844.
[33] D. J. Christopher, J. Yarwood, P. S. Belton, B. P. Hills, *J. Colloid Interface Sci.* **1992**, *152*, 465 – 472.
[34] H. R. Wyss, M. Falk, *Can. J. Chem.* **1970**, *48*, 607 – 617.

Manuscript received: November 23, 2017
Revised manuscript received: December 27, 2017
Version of record online: February 8, 2018